HHS Public Access

Author manuscript

Brain Behav Immun. Author manuscript; available in PMC 2016 August 01.

Published in final edited form as:

Brain Behav Immun. 2015 August ; 48: 301–312. doi:10.1016/j.bbi.2015.04.020.

Postnatal TLR2 activation impairs learning and memory in adulthood

Ravit Madar[1,2], **Aviva Rotter**[1,2], **Hiba Waldman Ben-Asher**[1], **Mohamed R. Mughal**[3], **Thiruma V. Arumugam**[4], **WH Wood 3rd**[3], **KG Becker**[3], **Mark P. Mattson**[3,5], and **Eitan Okun**[1,2]

[1] The Mina and Everard Goodman faculty of Life sciences, Bar-Ilan University, Ramat Gan, 52900, Israel

[2] The Leslie and Susan Gonda Multidisciplinary Brain Research Center, Bar-Ilan University, Ramat Gan, 52900, Israel

[3] Laboratory of Neurosciences, National Institute on Aging Intramural Research Program, Baltimore, Maryland 21224, USA

[4] Department of Physiology, Yong Loo Lin School of Medicine, National University of Singapore, Singapore

[5] Department of Neuroscience, Johns Hopkins University School of Medicine, Baltimore, MD 21205

Abstract

Neuroinflammation in the central nervous system is detrimental for learning and memory, as evident form epidemiological studies linking developmental defects and maternal exposure to harmful pathogens. Postnatal infections can also induce neuroinflammatory responses with long-term consequences. These inflammatory responses can lead to motor deficits and/or behavioral disabilities. Toll like receptors (TLRs) are a family of innate immune receptors best known as sensors of microbial-associated molecular patterns, and are the first responders to infection. TLR2 forms heterodimers with either TLR1 or TLR6, is activated in response to gram-positive bacterial infections, and is expressed in the brain during embryonic development. We hypothesized that early postnatal TLR2-mediated neuroinflammation would adversely affect cognitive behavior in the adult. Our data indicate that postnatal TLR2 activation affects learning and memory in adult mice in a heterodimer-dependent manner. TLR2/6 activation improved motor function and fear learning, while TLR2/1 activation impaired spatial learning and enhanced fear learning. Moreover, developmental TLR2 deficiency significantly impairs spatial learning and enhances fear learning, stressing the involvement of the TLR2 pathway in learning and memory. Analysis of the transcriptional effects of TLR2 activation reveals both common and unique transcriptional

*** Correspondence:** Eitan Okun, Ph.D., Senior Lecturer. The Leslie and Susan Gonda multidisciplinary brain research center. The Mina and Everard Goodman Faculty of Life sciences. Building 901, room 315. Bar Ilan University. Ramat Gan, 52900. Israel. Phones: +972-(0)3-7384670 (Laboratory), +972-(0)3-7384671 (Office), +972-(0)3-5352184 (Fax), eitan.okun@biu.ac.il.

programs following heterodimer-specific TLR2 activation. These results imply that adult cognitive behavior could be influenced in part, by activation or alterations in the TLR2 pathway at birth.

Keywords

Toll-like receptors; TLR2; Hippocampus; Spatial learning; Morris water maze; Fear conditioning; Cognition

Introduction

Toll like receptors (TLRs) are a family of type-I trans-membrane receptors best known as sensors of microbial-associated molecular patterns (MAMPs) by cells of the innate immune system (Kawai and Akira, 2007). Binding of MAMPs to TLRs typically activates signaling cascades that result in production of inflammatory cytokines/chemokines (Takeda and Akira, 2004). Activation of TLRs in the central nervous system (CNS) by MAMPs at different developmental stages (e.g.: embryonic, postnatal or adults) results in numerous effects, including impairment of various aspects of learning and memory in a neuroinflammation-dependent manner (Okun et al., 2011). Neuroinflammation in the CNS is a detrimental process for learning and memory (Hao et al., 2010). This insight draws from epidemiological studies linking developmental defects and maternal exposure to harmful pathogens. Such exposures could be either direct or indirect, affecting the intrauterine environment (Heindel, 2006). Indeed, maternal infection, whether local within the reproductive tract or a systemic subclinical infection may lead to both maternal and/or fetal inflammatory responses. These inflammatory responses can lead to motor deficits and/or behavioral disabilities (Rees et al., 2008). TLRs are heavily implicated in CNS neuroinflammation, as numerous MAMPs and tissue damage-associated molecular patterns (DAMPs) were reported to activate TLRs during infection and tissue damage (Mallard, 2012). TLR2 forms heterodimers with either TLR1 or TLR6 and different lipopeptides are thought to activate each heterodimer (Buwitt-Beckmann et al., 2006) with no apparent differences in the transcriptional outcomes (Farhat et al., 2008). FSL-1 (Pam2CGDPKHPKSF) is a synthetic lipoprotein (LP) derived from *Mycoplasma salivarium*. Mycoplasmal LPs, such as FSL-1, contain a diacylated cysteine residue, whereas bacterial LP contains a triacylated cysteine residue. FSL-1 is recognized by the TLR2/6 heterodimer, whereas bacterial LPs such as Pam3CysSerLys4 (Pam3CSK4) are recognized by the TLR2/1 heterodimer (Long et al., 2009). The interaction between TLR2 heterodimers and lipoproteins is governed by 4 different interaction types (Kang et al., 2009), which dictate its heterodimer binding partner. As a result, while FSL-1 and Pam3CSK4 bind different TLR2 heterodimers with strong affinity, both are probably capable of binding other heterodimers albeit with significantly lower affinity in-vivo. Postnatal exposure of mouse pups to TLR2 activation, between postnatal day (PND)-3 and PND11 with the synthetic lipopeptide Pam3CysSerLys4 (Pam_3CSK_4), displayed increased levels of interleukin (IL)-1β, IL-6, chemokine (C-X-C motif) ligand 1, and monocyte chemoattractant protein-1 in the brain. These mice also exhibited decreased volume of cerebral gray matter, and white matter in the forebrain at PND12, but no cognitive deficit was found at PND53 (Du et al., 2011). Despite this, the impact of postnatal TLR2 activation on the various aspects of

hippocampus-dependent learning and memory remains unclear. Here we provide evidence that early postnatal exposure to TLR2 activation confers long-term effects on hippocampus-dependent cognitive spatial and fear learning as well as on motor functions in a TLR2-heterodimer dependent manner during adulthood. These effects are correlated with immune- and extracellular matrix- related transcriptional changes.

Materials and methods

Animals

Congenic wild-type mice ($TLR2^{+/+}$, B6.129) and $TLR2^{-/-}$ mice (B6.129-Tlr2(tm1Kir)/J) were purchased from Jackson Laboratories (Bar Harbor, ME), and bred in-house to generate pups for this study. Animal care and experimental procedures followed NIH guidelines and were approved by the National Institute on Aging Animal Care and Use Committee.

Postnatal injections

For cerebral microinjections of endotoxin-free phosphate buffered saline (PBS) or the TLR2 ligands, Pam_3CSK_4 or FSL-1, P0 pups were placed on an ice-cooled plastic surface. The brain of each embryo was visualized with transillumination and the injections were performed using a glass capillary pipette (75–125 μm outer diameter with beveled tip) driven either by a Sutter micromanipulator (Suttor Instrument Company, Novato, CA, USA) equipped with a 20 μl Hamilton gas-tight syringe or a nitrogen-fed microinjector (Harvard Apparatus, PL1-100). Each pup was hand-held on top of the ice-cooled plastic surface, and a single 0.5 μ l bolus of either saline or 0.07 mg/kg of Pam3CSK4 or FSL1 (both dissolved in endotoxin-free PBS) was injected during 2 minutes to each hemisphere. This dose was previously determined by us to affect central neuroinflammation in late embryonic stages (Okun et al., 2010b)). A total of 41 $TLR2^{+/+}$ pups were injected with PBS, 33 $TLR2^{+/+}$ pups were injected with Pam_3CSK_4, 38 $TLR2^{+/+}$ pups were injected with FSL1, 33 $TLR2^{-/-}$ were injected with PBS and 31 $TLR2^{-/-}$ pups were injected with Pam3CSK4, and 26 $TLR2^{-/-}$ pups were injected with FSL1.

Behavioral testing

Rotarod test

Rotarod tests were performed at 6 weeks following birth (Figure 1) using the ENV-577M system (Med-associates, St. Albans, VT, USA). Rotarod acceleration was set to 4-40 revolutions per minute (RPM) over a period of 5 minutes. Mice were placed on the rotarod for three 5-minute trials with 15 minutes to rest between trials. Both the number of falls within 5 minutes and RPM at first fall were recorded and averaged.

Exploratory behavior

The open field tests were performed at 7 weeks following birth (1 week following completion of the rotarod tests, Figure 1). Exploratory behavior was assessed in the open field arena using the MED-OFA-MS system (Med Associates, St Albans, VT, USA) placed inside sound-attenuating boxes (model MED ENV-022V; Med Associates, St Albans, VT, USA). Animals were placed in the center of an open field (40.6 cm × 40.6 cm) and

exploration was assessed for 15 min. Cages were cleaned with 40% ethanol following each session. The peripheral 10.16 cm of the zone were considered as the peripheral zone and the central 20.32 cm were considered as the central zone. All open field tests were conducted under a light intensity of 400 lux. Open field-testing were conducted 6 weeks following birth (Figure 1A).

Spatial learning

To evaluate spatial learning and memory, mice were tested in the Morris water maze (MWM). The MWM task was performed at 12 weeks following birth (Figure 1). To test for spatial reference (long-term) memory, mice were trained in a water-filled pool (160 cm diameter) for 5 consecutive days, 4 trials per day, with spatial cues on the walls of the room. The cues (see (Okun et al., 2010a) for details) were black and white only, to reduce possible effects of color discrimination capabilities between the different treatments. The platform (rectangular platform, 153 cm^2 area) was hidden 0.5 cm below the water surface, at a constant location with mouse starting points changed every trial to avoid track memorization. When trials ended, either when the mouse had found the platform or when 60 seconds passed, mice were allowed to rest on the platform for 60 seconds. Latency to reach the platform, swimming distance, swimming speed and mean distance from the platform were recorded automatically by the Anymaze video tracking system (Stoelting Co, Wood Dale, IL, USA). Twenty-four hours following training, mice were subjected to a probe test, to evaluate memory retention. In this test, the platform was removed, and mice were allowed to swim for 30 s, and time the mice spent in each quadrant was measured. All tests were conducted under 20 lux illumination to reduce stress to the mice. In all the MWM tests, mice that exhibited passivity or a thigmotaxic swimming pattern were excluded from analysis (Okun et al., 2012). Water temperature was maintained at 27 ± 0.5 °C and was made opaque using nontoxic white paint. MWM tests were conducted 12 weeks following birth (Figure 1A). Mice exhibiting passive behavior in the pool (determined by both swim duration >52 s, average swim speed <0.13m/s and mean distance from the platform >0.41m) were excluded from analysis.

Fear conditioning

The fear-learning paradigm was conducted 2 weeks following completion of the MWM spatial task. Before testing, mice were first habituated to the testing room for 3 h/day for 3 days. In the training session, mice were placed in a contextual conditioning chamber (model MED VFC-NIR-M; Med Associates, St Albans, VT, USA) placed inside sound-attenuating boxes (model MED ENV-022V; Med Associates, St Albans, VT, USA). The conditioning chambers contained a metal grid on the floor (context A) and mice were allowed to explore the chamber for 2 min. At the end of 2 min mice were subjected to three sessions of audio tone (CS, conditioned stimulus) and foot shock (US, unconditioned stimulus). Audio tone (5 kHz, 70 dB) was on for 30 s, followed immediately by a 0.5-mA, 2-s foot shock from the metal grid floor. Thirty seconds separated each session. Foot shock intensity was determined in a preliminary test on a separate cohort of animals for the minimal applicable intensity to achieve a minimal freezing threshold of 40% during contextual fear. On the following day, in the contextual fear session (context A), mice were returned to the conditioning chamber for 5 min without any shock or audio tone. The percentage of time freezing was recorded

and used as an index of contextual memory. In the cued conditioning (conducted 3 h following contextual conditioning) mice were returned to the chamber but in a different context (context B). Context B was comprised of plastic triangle inserted to the cage coupled with plastic flooring placed underneath the triangular plastic insert. Mice were allowed to explore the chamber for 5 min without any audio tone. Following this, five audio tones were played for 30 s each. The percentage of time freezing until and after the audio tones was recorded and used as an index of cued memory. In all fear conditioning tests, cages were cleaned with ethanol between tests. Fear conditioning testing was conducted 12 weeks following birth (Figure 1A).

Cortical neuronal cell cultures

Dissociated cell cultures of cortical fragments were established from 18-day Sprague-Dawley rat embryos as previously described (Mattson and Kater, 1988). Neurons were plated on polyethylenimine (PEI) (0.005%)-coated 60 mm plastic dishes- and were maintained with Neurobasal medium supplemented with B27 (1:50, v:v) and arabinose-c (ara-c, 1μM, Sigma, USA) to eliminate astrocyte contamination. In all experiments, TLR2 ligands were applied for 24 hr.

Neuronal Progenitor Cell cultures

Neuronal progenitor cells (NPC) from the cortex were propagated as free-floating aggregates to promote proliferation of neural stem and progenitor cells prior to use in experiments. In brief, the dorsal telencephalon from E15 mouse embryos was isolated, mechanically dissociated, and cells were seeded at a density of 200,000/ml in a T75 flask containing Dulbecco's modified Eagle's medium/Ham's F-12 medium supplemented with B27 (1:50; Invitrogen), epidermal growth factor (EGF), and fibroblast growth factor 2 (FGF2) (both at 20 ng/ml; R&D Systems Inc). Growth factors were replenished every 3 days in culture. After neurospheres were grown for 7 days in culture the cells were induced for differentiation. To induce differentiation, growth factors were withdrawn and neurospheres were plated on polyethyleneimine (Sigma) coated dishes with the presence of 10% fetal calf serum.

Quantitative real-time PCR

RNA from either neuronal cultures or the cerebral cortex of P0 pups, was extracted using TRIzol Reagent (Ambion, Life Technologies, CA, USA). Complementary DNA (cDNA) was generated using Revert Aid H minus first strand cDNA synthesis kit (Thermo Scientific, Lithuania). The resulting cDNA was diluted 1:5 in nuclease-free water and stored in aliquots at −80 °C until used. RT-PCR reactions were performed using Fast SYBR Green Master Mix (Applied Biosystems, CA, USA) in a StepOnePlus instrument (Applied Biosystems, CA, USA). Primers were calibrated and negative control was performed for each primer pair. Samples were measured in triplicates and values were normalized according to mRNA levels of the β-Actin housekeeping gene. Quantification was assessed at the logarithmic phase of the PCR reaction using $2^{-\Delta\Delta CT}$ method as described previously (Livak and Schmittgen, 2001).

Gene-specific primers are listed in the following table:

Gene	Primers	Annealing Temp (°C)	Amplicon size (bp)	Species
Lcn2	Forward 5′ GGGCTGTCGCTACTGGATCA Reverse 5′ TGTACCTGAGGATACCTGTGCATATT	58.25	**90**	**Ms**
Lcn2	Forward 5′ GACCAGTTTGCCATGGTA Reverse 5′ CAGTCAGCCACGCTCA	52	**216**	**Rat**
Tf	Forward 5′ TGGCTACGTAGGCGCATTC Reverse 5′ TCCGGCAAGACCTCAAATATG	56.3	**90**	**Ms**
Tf	Forward 5′ GGTGAAGAAGGGAACAGA Reverse 5′ GACACAGCTGGGGGAA	51	**214**	**Rat**
Cxcl1	Forward 5′ TGCACCCAAACCGAAGTCAT Reverse 5′ TTGTCAGAAGCCAGCGTTCAC	57.65	**177**	**Ms**
Cxcl1	Forward 5′ ATGGCGTCTGTCTGGTGAA Reverse 5′ GTCCTTTGAACTTCTCTGTCCT	50	520	**Rat**
Timp1	Forward 5′ GCCCTTCGCATGGACATTTA Reverse 5′ ATGGTATCTCTGGTGTGTCTCTAGGA	56.9	**90**	**Ms**
Timp1	Forward 5′ GGGTTCCCCAGAAATCATCG Reverse 5′ CAGTGTTCAGGCTTCAGCTT	54	**515**	**Rat**
C1r	Forward 5′ GACCAGCTCCAGATCTACGC Reverse 5′ GGGCACTTGATGGTTTCAGT	56.45	**173**	**Ms**
C1r	Forward 5′ GCAAAGGCCTCCAGAC Reverse 5′ TCTCTCCTTCCTCTTCGT	50	**517**	**Rat**
Nfkbia	Forward 5′ TGGCCAGTGTAGCAGTCTTG Reverse 5′ GACACGTGTGGCCATTGTAG	56.75	90	Ms, Rat
Il17rb	Forward 5′ CCATCCCTCCAGATGACAAC Reverse 5′ GCTCCTTCCTTGCCTCCAAGTTA	57.1	122	Ms
Il17rb	Forward 5′ GATCTACCTAACTTGGAGGCAAG Reverse 5′ GTAGCCTTGAGAAGTTCTGTGT	53	525	Rat
C1s	Forward 5′ GTGGTGACGATGCAGAGAGA Reverse 5′ GCCCCATTAGGTCAGTTTGA	55.75	193	Ms
C1s	Forward 5′ AACCCAGAGCAATACTCTTG Reverse 5′ TGATACTCTCCGCCTTCTTC	50	420	Rat
Ccl2	Forward 5′ GGCTGGAGAGCTACAAGAGG Reverse 5′ ATGTCTGGACCCATTCCTTC	55.8	117	Ms
Ccl2	Forward 5′ CCCACTCACCTGCTGCT Reverse 5′ ACAGAAGTGCTTGAGGT	50	330	Rat
Tuj1	Forward 5′ CGC ATC ATG AAC ACC TTC AG Reverse 5′ ACA GGC AGC CAT CAT GTT C	54	426	Ms, Rat
S100b	Forward 5′ TGTTACTCGGACACTGAAG Reverse 5′ TTCCTGCTCCTTGATTTCC	51	218	Ms
S100b	Forward 5′ CTACACTAGGTATTCCTGTG Reverse 5′ GGGTGTGGGTGATAGGT	50	317	Rat
Gfap	Forward 5′ GTGTCAGAAGGCCACCT Reverse 5′ AAGGAAGGGGAGCACTG	54	217	Rat
Gfap	Forward 5′ CAACTGCAGGCCTTGAC Reverse 5′ CAGGGCTAGCTTAACGT	51	216	Ms
Mbp	Forward 5′ GGATTCAAGGGGGCCTA Reverse 5′ AGAGAAGACCCCGAGGA	53	317	Rat

Gene	Primers	Anneali ng Temp (°C)	Amplicon size (bp)	Species
Mbp	Forward 5′ ATCTCCCATGGCGAGAC Reverse 5′ GTAGGGGTGAACTTGGAAG	52	319	Ms
Tlr1	Forward 5′ ATG ATT CTG CCT GGG TGA AG Reverse 5′ TCT GGA TGA AGT GGG GAG AC	53	174	Ms
Tlr1	Forward 5′ TACCCTGAACAACGTGGACA Reverse 5′ ATCGACAAAGCCCTCAGAGA	54	165	Rat
Tlr2	Forward 5′ CTC CCA CTT CAG GCT CTT TG Reverse 5′ AGG AAC TGG GTG GAG AAC CT	53	217	Ms
Tlr2	Forward 5′ CGAAAAGAGCCACAAAACTGT Reverse 5′ CATTATCTTGCGCAGTTTGC	52	189	Rat
Tlr6	Forward 5′ ACACAATCGGTTGCAAAACA Reverse 5′ GGAAAGTCAGCTTCGTCAGG	50	178	Ms
Tlr6	Forward 5′ TGGCCCGAAAACCTTCTTCTCAACGGA Reverse 5′ GGGGCTTTCCTCTGTCTCTA	51	593	Rat
Tlr10	Forward 5′ GAACTCTATCTGGCCCACCA Reverse 5′ CACACCTTCCCCTTGTGTCT	51	235	Rat

Gene abbreviations: *Lcn2,* lipocalin2; *Tf,* transferrin; *Cxcl1,* chemokine (C-X-C motif) ligand 1; *Timp1,* tissue inhibitor of metalloproteinase-1; *C1r,* Complement component 1R; *Nfkbia,* NF-Kappa-B Inhibitor Alpha; *Il17rb,* Interleukin-17 receptor B; *C1s,* Complement component 1S; *Ccl2,* chemokine (C-C motif) ligand 2; *Tuj1,* Neuron-specific beta-III Tubulin; *S 100b,* S100 calcium binding protein B; *Mbp,* Myelin basic protein; *Gfap,* glial fibrillary acidic protein; *Tlr,* Toll-like receptor.

Illumina oligonucleotide microarray

Total RNA was used to generate biotin labeled cRNA using the Illumina TotalPrep RNA Amplification Kit (Ambion; Austin, TX, cat #IL1791). In short, 0.5 μg of total RNA was first converted into single-stranded cDNA with reverse transcriptase using an oligo-dT primer containing the T7 RNA polymerase promoter site and then copied to produce double-stranded cDNA molecules. The double stranded cDNA was cleaned and concentrated with the supplied columns and used in an overnight in vitro transcription reaction where single-stranded complementary RNA (cRNA) was generated and labeled by incorporation of biotin-16-UTP. A total of 0.75 μg of biotin-labeled cRNA was hybridized at 58 °C for 16 h to Illumina's Sentrix MouseRef-8 Expression Bead-Chips (Illumina, San Diego, CA). Each BeadChip has 24,000 well-annotated RefSeq transcripts with approximately 30-fold redundancy. The arrays were washed, blocked and the labeled cRNA was detected by staining with streptavidin-Cy3. The arrays were scanned using an Illumina BeadStation 500× Genetic Analysis Systems scanner and the image data extracted using the Illumina BeadStudio software, Version 3.0.

Statistical analysis

Analysis of all behavioral tests included both males and females as no statistically significant differences were observed between genders. Analyses of the open field, MWM and fear-conditioning experiments were performed using two-way analysis of variance (ANOVA) repeated measures with a Bonferroni post-hoc test. Analysis of rotarod experiments was done using one-way ANOVA. Statistical analysis was performed using Prizm 5 (Graphpad, USA). Results are expressed as mean ± S.E.M.

Microarray data analysis

The data from all arrays were first subjected to background correction by GenomeStudio software (Illumina, Inc., San Diego, CA). The rest of the analysis was performed in Partek® Genomics Suite software, version 6.6 Copyright © 2012 Partek Inc., St. Louis, MO, USA. Normalized data from two to six biological and technical replicates of control and treated cells were analyzed to identify genes whose expression was up- or down-regulated by an arbitrary cutoff of at least 1.8 fold, and had a P-value < 0.05 in all replicates when testing for differential expression (ANOVA test).

Gene interaction analysis

We generated networks of highly interconnected proteins using the STRING (Search Tool for the Retrieval of Interacting Genes, Heidelberg, Germany) 9.1 database (Franceschini et al., 2013). The Gene Ontology (GO) biological processes and the Kyoto Encyclopedia of Genes and Genomes (KEGG) pathways associated with the up- and down-regulated genes were retrieved from the STRING enrichment analysis tool (p-value<0.05).

Results

Postnatal TLR2/6 activation improves motor function in adult TLR2$^{+/+}$ but not TLR2$^{-/-}$ mice

Central postnatal TLR2/6 activation with FSL1 in TLR2$^{+/+}$ increased the time mice spent on the rotating rod (260 ± 13 seconds in FSL1-treated mice vs. 217 ± 9.3 seconds in PBS-treated mice; P=0.0078, two-way ANOVA with multiple comparisons; Figure 2A) and decreased the number of falls from the rod (0.67 ± 0.22 in FSL1-treated mice vs. 4.1 ± 0.65 in PBS-treated mice; P=0.002, two-way ANOVA with multiple comparisons; Figure 2B). Treatment of mice with the TLR2/1 ligand Pam3CSK4 did not affect time on the rotarod or number of falls in either TLR$^{+/+}$ or TLR$^{-/-}$ mice (Figure 2A, B). These data suggest that central postnatal TLR2/6 but not TLR2/1 activation improves motor learning during adulthood in TLR2$^{+/+}$ mice. No baseline differences in motor learning or coordination were noted between TLR2$^{-/-}$ and TLR2$^{+/+}$ mice in either time spent on the rod or number of falls (P>0.05) (Figure 2A, 2B).

TLR2 deficiency but not postnatal TLR2 activation affects exploratory behavior

In addition to motor function, another behavioral trait, which can affect the interpretation of cognitive behavior, is exploratory motivation. To test for differences in exploratory behavior, mice were placed in an open field arena, and walking distance, number of crosses between the center and peripheral zones, and time spent in each zone were measured (see methods for zone descriptions). TLR2 activation had no effect on TLR2$^{+/+}$ mice in walking distance (P>0.05, Figure S1A), zone entries (P>0.05, Figure S1B) and time spent in each zone (P>0.05, Figure S1C). Similar results were obtained for TLR2$^{-/-}$ mice (walking distance, P>0.05 Figure S1D; zone entries, P>0.05 Figure S1E; or time spent in each zone, P>0.05 Figure S1F). When baseline differences between TLR2$^{-/-}$ and TLR2$^{+/+}$ mice were compared, significant differences were observed in walking distance (P<0.0001, $F_{3,1040}$=264.69, two-way repeated measures (RM)-ANOVA; Figure 3A) and number of center to periphery zone crosses (P<0.0001, $F_{3,520}$=27.09, two-way RM-ANOVA; Figure

3B). Time spent in each zone was not different between the two strains (P>0.05; Figure 3C). This suggests that while TLR2$^{-/-}$ mice are mildly less active than TLR2$^{+/+}$ mice, they do not exhibit impaired anxiety.

Postnatal TLR2/1 but not TLR2/6 heterodimer activation impairs spatial learning in adulthood

In order to assess the long-term effects of postnatal exposure to TLR2 activation on spatial learning, we tested mice 12 weeks following postnatal exposure to PBS, the TLR2/1 ligand Pam3CSK4 or the TLR2/6 ligand FSL1 in the MWM, a dorsalhippocampus dependent spatial learning and memory task. A significant day effect was observed in latency to reach the platform for PBS- and TLR2/6 ligand-treated TLR2$^{+/+}$ mice (P<0.0001, $F_{2,400}$=10.22, two-way RM-ANOVA, Figure 4A). However, compared with these mice, the latency of TLR2$^{+/+}$ treated with the TLR2/1 ligand to reach the platform was greater on days 2-4 ($F_{2,400}$=11.58, two-way RM-ANOVA, Figure 4A). Swim speed did not differ between the groups (P>0.05, Figure 4B). Although a day effect was observed for the three groups in swim distance ($F_{2,400}$=6.15, two-way RM-ANOVA, Figure 4C), no difference was observed between groups. While PBS-treated mice exhibited memory retention in the probe trial (P=0.0028, one-way ANOVA, Figure S2A), FSL1-and Pam3CSK4-treated mice failed to exhibit such memory retention (P>0.05, one way ANOVA, Figures S2B and S2C).

These data suggest that TLR2$^{+/+}$ mice exposed to postnatal TLR2/1 activation exhibited slower learning of a spatial cognitive task compared with mice receiving PBS or a TLR2/6 ligand. Neither TLR2/1 nor TLR2/6 postnatal activation had an effect on the performance of TLR2$^{-/-}$ mice in the MWM compared with PBS-treated TLR2$^{-/-}$ mice as measured by latency to reach the hidden platform (P>0.05, Two-way RM-ANOVA, Figure S3A), swim speed (P>0.05, Two-way RM-ANOVA, Figure S3B) or swim distance (P>0.05, Two-way RM-ANOVA, Figure S3C). As a result, TLR2$^{-/-}$ mice treated with PBS, FSL1-or Pam3CSK4- failed to exhibit spatial memory retention (P>0.05, one way ANOVA, Figures S2D-F). In fact, TLR2 deficient mice exhibited a higher latency to reach the platform compared to TLR2$^{+/+}$ mice ($F_{1,237}$=43, P<0.0001, Two-way-RM ANOVA, Figure 4E). TLR2$^{-/-}$ mice also exhibited slower swim speed ($F_{1,237}$=50, P<0.0001, Two-way-RM ANOVA, Figure 4F) and longer swimming distance ($F_{1,237}$=8.4, P<0.0001, Two-way RM-ANOVA, Figure 4G). Thus, performance of TLR2$^{-/-}$ mice in the MWM task was impaired compared with TLR2$^{+/+}$ mice. Of notice, TLR2$^{+/+}$ mice treated with Pam3CSK4, FSL1 or PBS exhibited similar swim speed throughout training days 1-5 (Figure 4B). As a result, swim speed did not affect their performance in this task. When compared with TLR2$^{+/+}$ mice, TLR2$^{-/-}$ mice also exhibited similar swim speeds (Figure 4E). Therefore, the higher latency of TLR2$^{-/-}$ mice in reaching the platform could not be explained by altered swim speed.

Taken together, these data suggest that both developmental TLR2 deficiency and neonatal TLR2/1 but not TLR2/6 activation impair spatial learning in adulthood, highlighting the importance of the TLR2 pathway to spatial learning.

Central postnatal TLR2 activation enhances contextual and cued fear learning in adult TLR2$^{+/+}$ mice

The hippocampus is a central hub for multiple types of learning behaviors. As spatial learning was affected by early post-natal TLR2 activation, we sought to test whether additional hippocampus-dependent cognitive domains such as fear learning (Maren, 2008) are affected by postnatal TLR2 activation. Fear conditioning is a Pavlovian task shown to mostly involve the ventral hippocampal formation, the amygdala and the prefrontal cortex (Liu et al., 2011). To test whether TLR2 activation in the CNS of neonate pups confers long-term effects on fear learning during adulthood, we utilized the fear-conditioning paradigm. Central postnatal TLR2 activation with either Pam3CSK4 or FSL1 in TLR2$^{+/+}$ mice had no effect on the rate of acquiring the association between the tone-shock pairs ($P>0.05$, Figure 5A). However, both activation of TLR2/1 and TLR2/6 resulted in increased freezing behavior in response to the context of the fear ($F_{2,504}=18.81$, $p<0.0001$, two-way ANOVA; Figure 5B). In addition, when the mice were exposed to the tone cue under a different context, a significantly higher freezing behavior was recorded in mice exposed to either TLR2/1 or TLR2/6 ligands compared with mice exposed to PBS ($F_{2,202}=8.72$, $p=0.0002$, two-way ANOVA; Figure 5C). These data suggest that postnatal TLR2 activation does not affect fear-memory acquisition, but enhances its expression in hippocampus- and amygdala-dependent tasks. TLR2 activation resulted in minimal non-specific effects in TLR2$^{-/-}$ mice. While no significant differences were noted in memory acquisition ($P>0.05$, Figure 5D), postnatal TLR2/6 but not TLR2/1 activation in TLR2$^{-/-}$ mice resulted in higher contextual freezing ($F_{2,83}=4.788$, $P=0.0108$, two way ANOVA, Figure 5E) but not cued fear ($p>0.05$, Figure 5F).

Similar to the impairment of spatial learning in TLR2$^{-/-}$ mice compared to TLR2$^{+/+}$ mice, TLR2 deficiency also resulted in significant alterations in fear learning. TLR2$^{-/-}$ mice exhibited more freezing during the acquisition phase ($F_{1,198}=21$, $p<0.0001$, two-way RM-ANOVA, Figure 5G), indicating enhanced acquisition of the tone-shock pairs compared with TLR2$^{+/+}$ mice. TLR2$^{-/-}$ mice also exhibited a significantly higher freezing percentage during the contextual fear phase compared to TLR2$^{+/+}$ mice ($F_{1,264}=39.63$, $p<0.0001$, Figure 5H). In the cued fear, TLR2$^{-/-}$ mice exhibited more baseline freezing compared to TLR2$^{+/+}$ mice and also greater cue-induced fear ($F_{1,66}=13.3$, $p=0.0005$, Figure 5I). These data suggest that TLR2$^{-/-}$ mice are hypersensitive to fear learning, as indicated by altered acquisition rate, and fear-memory retention, as indicated by greater contextual and cued fear expression.

mRNA for the TLR2/1 and TLR2/6 heterodimers components are expressed in NPC-derived neurons

To unravel a possible underlying mechanism for the effects of postnatal central TLR2 activation on adult cognitive learning, we assessed which components of the TLR2 heterodimer receptor complex are expressed in neurons. Mouse and rat NPC were grown and subsequently induced to differentiate into mixed or pure neuronal cultures (Figure 6A and 6B respectively). The mRNA of TLRs 1, 2 and 6 were expressed in TUJ1-sorted neurons differentiated from mouse or rat NPCs (Figure 6A and 6B respectively).

TLR2/1 and TLR2/6 activation in neurons drives an immune-related transcriptional response

Since both the mRNA for TLR1 and TLR6 were present in cortical neurons, we aimed at assessing whether activation of the two TLR2 heterodimers results in functionally different outcomes. To this end, RNA from neurons treated with the TLR2/6 ligand FSL1 and the TLR2/1 ligand Pam3CSK4 were analyzed using the Illumina rat gene array platform. Each experiment was repeated between two to six times (biological and technical replicates). Normalized data were used to identify genes whose expression was significantly up-or down- regulated (p value 0.05, ANOVA) with a magnitude exceeding a cutoff of 1.8 fold. Analysis of the degree of overlap between the genes affected by the Pam3CSK4 and the FSL1 groups showed that 36 genes were common to both FSL1 and Pam3CSK4 (Spearman correlation 0.83 with p value for the overlap of 1×10^{6}) (Figure 7A, Table 1). Gene ontology analysis of the 36 genes indicates that 18 of the 36 genes (50%) are immune-related transcripts. Other genes are related to iron homeostasis (2 transcripts), response to oxygen compounds (6 transcripts) and cell adhesion (2 transcripts). The number of uniquely regulated genes in FSL1 and Pam3CSK4-treated neurons was 55 and 8 respectively (Figure 7A, Tables 2 and 3). FSL1 induced unique changes in transcripts related to extracellular matrix (8 transcripts), cell adhesion (7 transcripts) and cell differentiation (12 transcripts). Extracellular matrix–related transcripts were also affected by Pam3CSK4 treatment (3 of 8 transcripts).

As our gene-array analysis revealed that both TLR2/1 and TLR2/6 activation induce significant expression of immune-related transcripts, we initially tested whether this was due to astrocyte contamination of the neuronal cultures or whether these genes were indeed expressed by neurons. Single-cell PCR performed on RNA from isolated neurons showed that neurons express the mRNA of a select list of immune-related transcripts found to be altered in the gene array analysis: *Timp1*, *Nfkbia*, *Cxcl1*, *C1s*, *Lcn2*, *Ccl2*, *Il17rb* and *Tf* (Figure 7B). Since these genes are expressed in neurons, we tested whether neuronal cultures depleted of glia by treatment with Ara-c exhibit up-regulation of these genes in response to TLR2/1 or TLR2/6 activation. Indeed, these immune-related genes were up-regulated by FSL1 and Pam_3CSK_4 (Figure 7C). To verify that this phenomenon also occurs in vivo, we injected P0 pups with Pam3CSK4, and extracted RNA from cortical tissues 24 hours later. Of the 9 immune-related genes validated in vitro, only 5 genes were validated in vivo (*C1s*, *C1r*, *Nfkbia*, *Lcn2* and *Tf* (Figure 8).

Discussion

The present study contributes a mechanistic insight into a body of evidence linking postnatal central infection and long-lasting cognitive impairments during adulthood. Our data indicates that TLR2-induced neuroinflammation in the neonatal brain differentially affects cognitive spatial and fear learning, as well as motor functions during adulthood in a TLR2-heterodimer specific manner.

TLR2 forms heterodimers with either TLR1 or TLR6. The MAMP Pam3CSK4 preferentially activates the TLR2/1 heterodimer; however, in the absence of TLR1, Pam_3CSK_4 also activates the TLR2/6 heterodimer with a lower affinity (Buwitt-Beckmann

et al., 2006). In the absence of TLR2, however, Pam3CSK4 does not activate TLR1 or TLR6 (Buwitt-Beckmann et al., 2006). While different MAMPs activate the TLR2/1 and TLR2/6 heterodimer complexes, the two-heterodimer complexes were thought to initiate an identical signaling cascade (Farhat et al., 2008). Therefore, to resolve whether a differential activation of the two heterodimers result in similar transcriptional and behavioral effects, we used Pam3CSK4 as a ligand to activate the TLR2/1 heterodimer complex, and FSL1 to activate the TLR2/6 heterodimer complex. A recent study (Du et al., 2011) showed that daily administration of a TLR2/1 ligand from PND 3 - 11 confers no effect on fear learning on PND 53. In contrast, our data indicate that exposure to TLR2/1 and TLR2/6 activation in newborn mice significantly increases contextual fear responses at 2 months after birth. These effects were not accompanied by abnormalities in open field behavior, indicating that the cognitive effects of early postnatal TLR2 activation were not the result of altered anxiety. This is further exemplified by the fact that only TLR2/1 activation impaired spatial learning while TLR2/6 had no such effect. Injecting a TLR2 ligand to $TLR2^{-/-}$ mice did not affect exploratory behavior, motor or spatial learning. However, TLR2/6 activation did increase contextual fear learning. The increased freezing exhibited by $TLR2^{-/-}$ mice does not seem to be dependent on context, as in both context dependent and context independent responses the baseline freezing was higher in $TLR2^{-/-}$ mice compared with $TLR2^{+/+}$ mice. These results suggest that in the absence of TLR2, receptors other than TLR1 or TLR6 could be activated and promote long-term effects on contextual but not cued fear learning.

Our data clearly indicates that TLR2 deficiency alters cognitive function. TLR2 deficient mice exhibit reduced exploratory behavior in the open field, blunted spatial learning capacity and an elevated fear response. Indeed, both TLR2/1 activation and a developmental deficiency of the TLR2 receptor similarly impaired spatial learning. However, the mechanisms behind the two effects probably differ. Developmental TLR2 deficiency does not seem to involve inflammatory mediators but may affect brain development during embryogenesis (Okun et al., 2011). Park and colleagues have recently linked TLR2 deficiency to schizophrenia-like behavior in mice (Park et al., 2015). In their study, TLR2 deficiency resulted in hyperlocomotion, reduced anxiety-like behavior and impaired spatial and fear learning and memory. In contrast, our data show that TLR2 deficiency does not affect motor function, reduces exploratory behavior while not affecting anxiety levels, enhances fear learning and memory and impairs spatial memory. It is difficult to interpret these contradictory results, however, it appears that the $TLR2^{-/-}$ mice used by Park et al. (2015) were on a mixed genetic background, whereas the wild type mice used by the authors were C57Bl/6 mice. In contrast, all the genotypes in the current study were on a congenic C57BL/6 background. Therefore, differences in animal behavior could be result of genetic background rather than TLR2 deficiency.

It was previously suggested that activation of the TLR2/1 and TLR2/6 heterodimers results in similar transcriptional outcomes (Farhat et al., 2008). Our validated gene array data indicate that while a significant transcriptional overlap exists in neurons exposed to TLR2/1 and TLR2/6 ligands, each heterodimer also triggers a distinct transcriptional program, exemplified by extracellular remodeling, cell adhesion and cell differentiation transcriptional programs by TLR2/6 activation, while TLR2/1 activation affects several genes related to extracellular matrix remodeling. Although several important immune-

related genes are differentially expressed in FSL1 and Pam3CSK4-treated neurons compared to controls (Table 1), no distinct mRNAs for pro-inflammatory cytokines appear to be driven by TLR2 activation in neurons. Although TLR2 activation is expected to drive expression of pro-inflammatory genes in immune cells, it appears that neurons exposed to PAMP-induced TLR activation, TLR2 included, do not respond in a nuclear-factor kappa-B-dependent (NFkB)-dependent manner (Okun et al., 2011). While the reason for this is unknown, the high levels of TLR2-induced *Nfkbia* expression (Table 1, Figures 7-8) by neurons both in vitro and in-vivo could provide a possible explanation for this. *Nfkbia*, Inhibits the activity of dimeric NFkB/REL complexes by trapping REL dimers in the cytoplasm through masking of their nuclear localization signals (Huxford et al., 1998). Therefore, our data raise the possibility that in neurons, expression of pro-inflammatory mediators is blunted following TLR2 activation due to *Nfkbia* expression. Of the 9 immune-related genes we observed to alter following TLR2/1 and TLR2/6 activation in vitro, only 5 genes (*C1s*, *C1r*, *Nfkbia*, *Lcn2* and *Ccl2*) exhibited similar changes following TLR2/1 activation in vivo. We conclude that these 5 validated genes indicate that neurons in-vivo also responded in a similar manner to TLR2 activation as did neurons in-vitro. We regard the genes that failed to validate as TLR2-mediated effects that occurred solely in neurons in vitro or transcriptional changes that were negated by glial cells in vivo.

While the data herein indicate the long-term effects of postnatal central infection, several factors need to be considered. First, when a pathogen infects the brain, more than one innate immune pathway is activated. For example, in addition to TLR2, members of the NOD-like receptors (NLRs) family of innate immune receptors, could be activated by bacterial-derived PAMPs (Feldman et al., 2015). In addition, the tissue damage caused by injection can present a source of DAMPs presented to the brain, unlike in a situation in which bacterial infection compromises the neonatal brain. Lastly, this study focuses on the outcomes of central rather than peripheral induction of neuroinflammation. Indeed, peripheral neonatal infection mildly affects spatial learning in adulthood (Cronise and Kelly, 2001; Wallace et al., 2010; Williamson and Bilbo, 2014), Our conclusions on the impact of central postnatal neuroinflammation on adult cognitive learning, however, cannot be extrapolated to peripheral infection in neonates.

Overall, our findings suggest that TLR2 is an important player in the plasticity of cognitive behavior, in that activation of TLR2 impairs certain cognitive functions, while enhancing others. Importantly, our findings demonstrate that a single exposure to a TLR2 ligand in the early postnatal period can cause long-lasting alterations in cognitive function, suggesting that exposure of infants to infectious agents that activate TLR2 might affect their learning and memory ability later in life.

Supplementary Material

Refer to Web version on PubMed Central for supplementary material.

Acknowledgements

This work was supported, in part, by the Intramural Research Program of the National Institute on Aging.

References

Buwitt-Beckmann U, Heine H, Wiesmuller KH, Jung G, Brock R, Akira S, Ulmer AJ. TLR1- and TLR6-independent recognition of bacterial lipopeptides. The Journal of biological chemistry. 2006; 281:9049–9057. [PubMed: 16455646]

Cronise K, Kelly SJ. Maternal urinary tract infection alters water maze performance in the offspring. Neurotoxicology and teratology. 2001; 23:373–379. [PubMed: 11485840]

Du X, Fleiss B, Li H, D'Angelo B, Sun Y, Zhu C, Hagberg H, Levy O, Mallard C, Wang X. Systemic stimulation of TLR2 impairs neonatal mouse brain development. PloS one. 2011; 6:e19583. [PubMed: 21573120]

Farhat K, Riekenberg S, Heine H, Debarry J, Lang R, Mages J, Buwitt-Beckmann U, Roschmann K, Jung G, Wiesmuller KH, Ulmer AJ. Heterodimerization of TLR2 with TLR1 or TLR6 expands the ligand spectrum but does not lead to differential signaling. Journal of leukocyte biology. 2008; 83:692–701. [PubMed: 18056480]

Feldman N, Rotter-Maskowitz A, Okun E. DAMPs as mediators of sterile inflammation in aging-related pathologies. Ageing research reviews. 2015

Franceschini A, Szklarczyk D, Frankild S, Kuhn M, Simonovic M, Roth A, Lin J, Minguez P, Bork P, von Mering C, Jensen LJ. STRING v9.1: protein-protein interaction networks, with increased coverage and integration. Nucleic acids research. 2013; 41:D808–815. [PubMed: 23203871]

Hao LY, Hao XQ, Li SH, Li XH. Prenatal exposure to lipopolysaccharide results in cognitive deficits in age-increasing offspring rats. Neuroscience. 2010; 166:763–770. [PubMed: 20074621]

Heindel JJ. Role of exposure to environmental chemicals in the developmental basis of reproductive disease and dysfunction. Seminars in reproductive medicine. 2006; 24:168–177. [PubMed: 16804815]

Huxford T, Huang DB, Malek S, Ghosh G. The crystal structure of the IkappaBalpha/NF-kappaB complex reveals mechanisms of NF-kappaB inactivation. Cell. 1998; 95:759–770. [PubMed: 9865694]

Kang JY, Nan X, Jin MS, Youn SJ, Ryu YH, Mah S, Han SH, Lee H, Paik SG, Lee JO. Recognition of lipopeptide patterns by Toll-like receptor 2-Toll-like receptor 6 heterodimer. Immunity. 2009; 31:873–884. [PubMed: 19931471]

Kawai T, Akira S. Signaling to NF-kappaB by Toll-like receptors. Trends in molecular medicine. 2007; 13:460–469. [PubMed: 18029230]

Liu CC, Crone NE, Franaszczuk PJ, Cheng DT, Schretlen DS, Lenz FA. Fear conditioning is associated with dynamic directed functional interactions between and within the human amygdala, hippocampus, and frontal lobe. Neuroscience. 2011; 189:359–369. [PubMed: 21664438]

Livak KJ, Schmittgen TD. Analysis of relative gene expression data using real-time quantitative PCR and the 2(-Delta Delta C(T)) Method. Methods. 2001; 25:402–408. [PubMed: 11846609]

Long EM, Millen B, Kubes P, Robbins SM. Lipoteichoic acid induces unique inflammatory responses when compared to other toll-like receptor 2 ligands. PloS one. 2009; 4:e5601. [PubMed: 19440307]

Mallard C. Innate immune regulation by toll-like receptors in the brain. ISRN neurology. 2012; 2012:701950. [PubMed: 23097717]

Maren S. Pavlovian fear conditioning as a behavioral assay for hippocampus and amygdala function: cautions and caveats. The European journal of neuroscience. 2008; 28:1661–1666. [PubMed: 18973583]

Okun E, Barak B, Saada-Madar R, Rothman SM, Griffioen KJ, Roberts N, Castro K, Mughal MR, Pita MA, Stranahan AM, Arumugam TV, Mattson MP. Evidence for a developmental role for TLR4 in learning and memory. PloS one. 2012; 7:e47522. [PubMed: 23071817]

Okun E, Griffioen K, Barak B, Roberts NJ, Castro K, Pita MA, Cheng A, Mughal MR, Wan R, Ashery U, Mattson MP. Toll-like receptor 3 inhibits memory retention and constrains adult hippocampal neurogenesis. Proc Natl Acad Sci U S A. 2010a; 107:15625–15630. [PubMed: 20713712]

Okun E, Griffioen KJ, Mattson MP. Toll-like receptor signaling in neural plasticity and disease. Trends Neurosci. 2011; 34:269–281. [PubMed: 21419501]

Okun E, Griffioen KJ, Son TG, Lee JH, Roberts NJ, Mughal MR, Hutchison E, Cheng A, Arumugam TV, Lathia JD, van Praag H, Mattson MP. TLR2 activation inhibits embryonic neural progenitor cell proliferation. J Neurochem. 2010b; 114:462–474. [PubMed: 20456021]

Park SJ, Lee JY, Kim SJ, Choi SY, Yune TY, Ryu JH. Toll-like receptor-2 deficiency induces schizophrenia-like behaviors in mice. Scientific reports. 2015; 5:8502. [PubMed: 25687169]

Rees S, Harding R, Walker D. An adverse intrauterine environment: implications for injury and altered development of the brain. International journal of developmental neuroscience : the official journal of the International Society for Developmental Neuroscience. 2008; 26:3–11. [PubMed: 17981423]

Takeda K, Akira S. TLR signaling pathways. Seminars in immunology. 2004; 16:3–9. [PubMed: 14751757]

Wallace KL, Lopez J, Shaffery JP, Wells A, Paul IA, Bennett WA. Interleukin-10/Ceftriaxone prevents E. coli-induced delays in sensorimotor task learning and spatial memory in neonatal and adult Sprague-Dawley rats. Brain research bulletin. 2010; 81:141–148.

Williamson LL, Bilbo SD. Neonatal infection modulates behavioral flexibility and hippocampal activation on a Morris Water Maze task. Physiology & behavior. 2014; 129:152–159. [PubMed: 24576680]

Research highlights

- TLR2 activation using TLR2/1 and TLR2/6 heterodimer specific ligands in neonates affects cognitive behavior in adulthood in a TLR2-heterodimer specific manner.
- Developmental TLR2 deficiency affects multiple cognitive traits in adulthood.
- Activation of TLR2/1 and TLR2/6 in neurons exerts differential gene expression

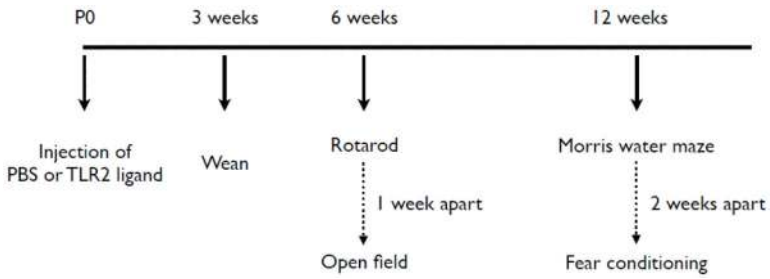

Figure 1. Experimental design

$TLR2^{+/+}$ mice (n = 112) and $TLR2^{-/-}$ (n = 90) mice were injected with PBS, FSL1 (a TLR2/6 ligand) or Pam3CSK4 (a TLR2/1 ligand) immediately after birth. At 3 weeks, pups were weaned, and at 6 weeks mice were tested in the open field to assess exploratory behavior and on the rotarod to assess their motor function. At 12 weeks, mice were tested for spatial and contextual fear learning.

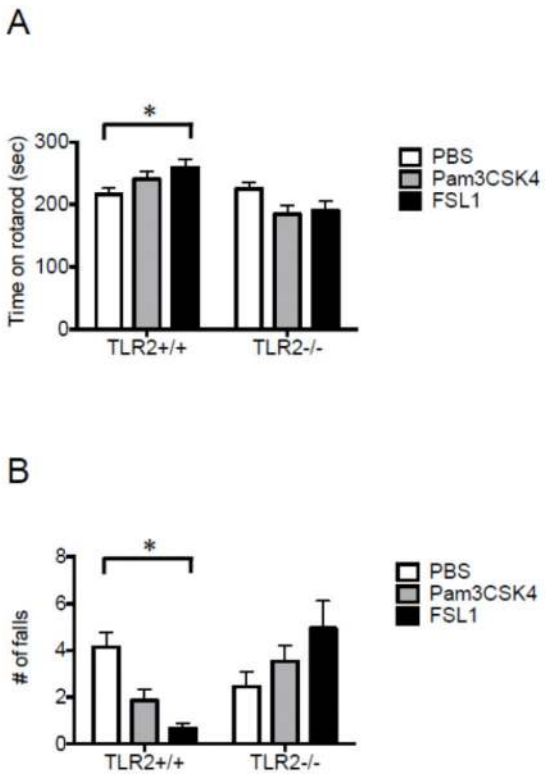

Figure 2. Central postnatal TLR2/6 but not TLR2/1 activation enhances motor performance in adult mice

TLR2$^{+/+}$ and TLR2$^{-/-}$ mice were injected with either PBS (n=41 and 33 respectively), the TLR2/6 ligand FSL1 (n=14 and 20 respectively), or the TLR2/1 ligand Pam3CSK4 (n=30 and 31 respectively), immediately after birth. At the age of 6 weeks, the mice were tested for motor function on the rotarod. (**A**) The average time mice spent on the rotating rod and (**B**) the number of falls from the rotarod was measured. *P<0.05.

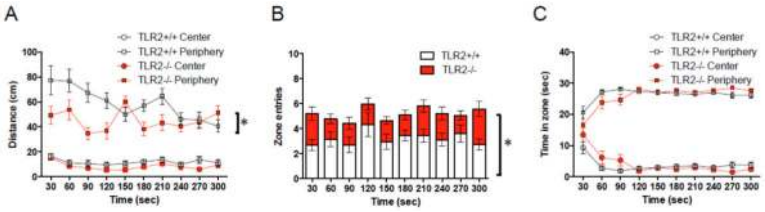

Figure 3. TLR2 deficiency reduces exploratory behavior in adult mice

$TLR2^{+/+}$ (n=42) and $TLR2^{-/-}$ (n=33) mice were injected with PBS immediately after birth. At the age of 6 weeks, the mice were placed for 5 minutes in the center of an open field under light intensity of 400 lux. Mouse activity was recorded and total walking distance, zone crosses between the peripheral and the center zones, and time in each zone, were compared between $TLR2^{+/+}$ and $TLR2^{-/-}$ mice (**A-C**). * P<0.05.

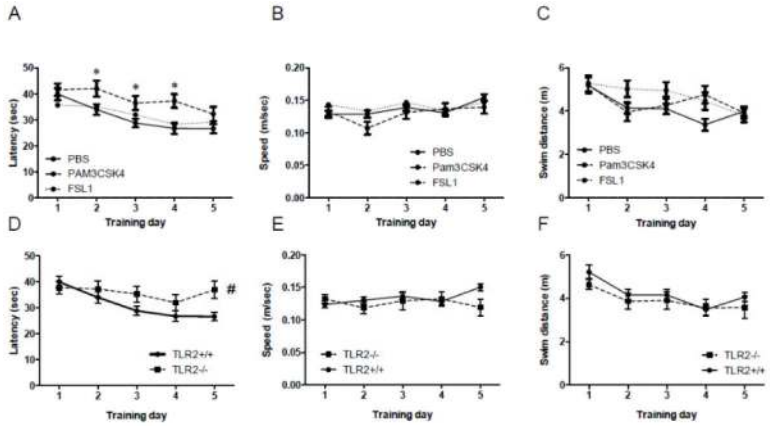

Figure 4. Central postnatal TLR2/1 activation in TLR2$^{+/+}$ mice and TLR2 deficiency impair spatial learning in adult mice

TLR2$^{+/+}$ were mice injected with either PBS (n=39), the TLR2/6 ligand FSL1 (n=37), or the TLR2/1 ligand Pam3CSK4 (n=30), immediately after birth. At the age of 12 weeks, the mice were tested for spatial learning ability in the MWM. The performance of each mouse was video-recorded and the goal latency, swim speed and swim distance were analyzed for TLR2$^{+/+}$ mice **(A-C).** A Direct comparison of TLR2$^{+/+}$ (n=39) and TLR2$^{-/-}$ (n=29) mice is shown in panels **(D-F)**. * P<0.05 on days 2-4 in Pam3CSK4- vs. PBS-treated mice. # P<0.05 when comparing TLR2$^{+/+}$ and TLR2$^{-/-}$ mice.

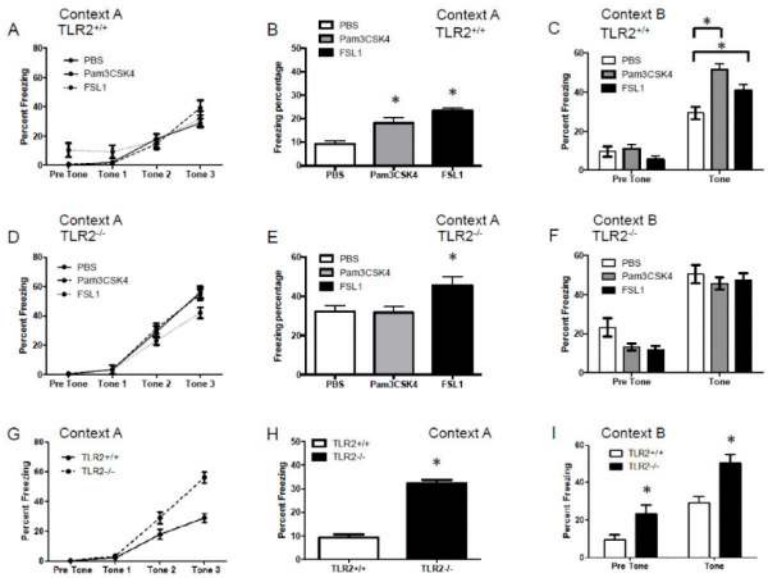

Figure 5. Central postnatal TLR2 activation and TLR2 deficiency enhance contextual and cued fear learning in adult mice

$TLR2^{+/+}$ and $TLR2^{-/-}$ mice injected with either PBS (n=39 and 29 respectively), the TLR2/6 ligand FSL1 (n=35 and 26 respectively), or the TLR2/1 ligand Pam_3CSK_4 (n=30 and 31 respectively), immediately after birth. At the age of 12 weeks, the mice were tested in the fear-conditioning paradigm. The performance of the mice during the acquisition phase, contextual fear and cued fear was analyzed for $TLR2^{+/+}$ mice **(A-C)** and $TLR2^{-/-}$ mice **(D-F)**. Direct comparison of PBS-treated $TLR2^{+/+}$ and $TLR2^{-/-}$ mice is shown in **(H-I)**. Contexts A and B indicate the context in which the mice were tested in. *P<0.05

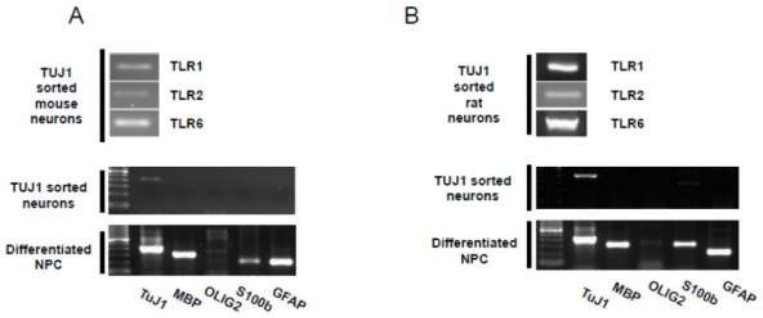

Figure 6. Neurons express mRNA for TLRs 1, 2 and 6

NPCs derived from **(A)** mouse and **(B)** rat embryos were differentiated into neurons, astrocytes and oligodendrocytes. The cells were then sorted using FACS into TUJ1-expressing cells and analyzed for expression of TLR 1, 2 and 6 mRNAs.

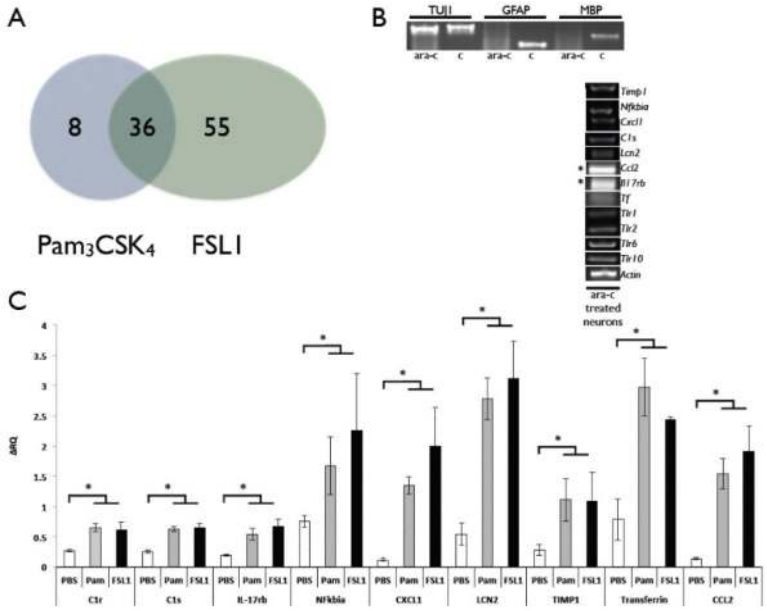

Figure 7. TLR2/1 and TLR2/6 heterodimer activation in glia-depleted cortical neurons in culture induces expression of immune-related genes

(A) Gene array analysis of FSL1- and Pam3CSK4-treated neurons resulted in 36 genes co-regulated by both treatments, 8 genes uniquely altered by Pam3CSK4, and 55 genes uniquely altered by FSL1 treatment. Cortical neurons derived from E18 rat embryos were treated with Ara-c to prevent growth of astrocytes in the culture. **(B)** Neuronal cultures exhibit high purity of neurons with negligible glial cells. These neurons express mRNA for *Timp1*, *Nfkbia*, *Cxcl1*, *C1s*, *Lcn2*, *Ccl2*, *IL17rb*, *Tf*, *Tlr1*, *Tlr2*, *Tlr6* and *Tlr10*. **(C)** FSL1 and Pam3CSK4-treated cortical neurons exhibit up regulation of the above genes. * P<0.05.

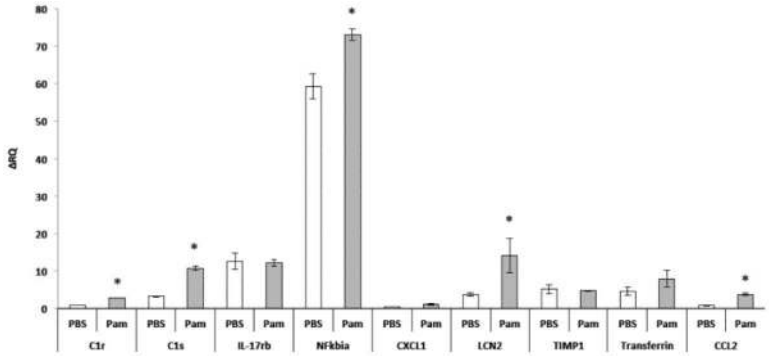

Figure 8. TLR2/1 activation in P0 mouse pups induces the expression of immune-related genes

P0 TLR2$^{+/+}$ mice were injected with Pam_3CSK_4 and were sacrificed after 24 hours. RNA was then extracted from the cortices of these pups and mRNA for *Timp1*, *Nfkbia*, *Cxcl1*, *C1s*, *Lcn2*, *Ccl2*, *IL17rb* and *Tf* was measured. * P<0.05.

Table 1

Genes significantly changed in both FSLl- and Pam_3CSK_4-treated cells.

Gene	Accession	Description	Fold change (treatment vs. control)	
			FSL1	Pam3CSK4
		Immune response		
Vcam1	*NM_012889.1*	Vascular cell adhesion molecule 1	2.15536	2.38354
Nfkbia	*NM_001105720*	Nuclear factor of kappa light chain gene enhancer in B-cells inhibitor, alpha	2.54205	2.77152
C3	*NM_016994*	Complement component 3	3.44035	3.38284
C1s	*NM_138900.1*	Complement component 1, s subcomponent	4.12182	3.61322
Cxcl1	*NM_030845.1*	Chemokine (C-X-C motif) ligand 1	7.54967	7.18406
Csf1	*NM_023981.4*	Colony stimulating factor 1 (macrophage)	2.07123	2.3566
Lgals3	*NM_031832.1*	Lectin, galactose binding, soluble 3	2.66067	2.44433
Ccl20	*NM_019233.1*	Chemokine (C-C motif) ligand 20	4.40416	4.26894
C1r	*NM_001134555*	Complement subcomponent 1, r precursor	2.79518	2.64204
Rt1-a1	*NM_001008827*	RT1 class Ia, locus A1	1.88943	1.81264
Icam1	*NM_012967.1*	Intercellular adhesion molecule 1	1.95994	2.03059
Ccl2	*NM_031530.1*	Chemokine (C-C motif) ligand 2	12.4705	9.34879
Lcn2	*NM_130741.1*	Lipocalin 2	35.5416	19.3122
Cfb	*NM_212466.3*	Complement factor B	3.19197	2.02654
Ccl7	*NM_001007612.1*	Chemokine (C-C motif) ligand 7	4.48606	3.55715
Il17rb	*NM_001107290*	Interleukin 17 receptor B	2.2991	1.87533
Chi3l1	*NM_053560*	Chitinase 3-like 1	3.5555	2.27651
Cd83	*NM_001108410*	CD83 antigen	2.25055	2.48039
		Iron homeostasis		
Cp	NM_012532	Ceruloplasmin (ferroxidase)	5.15266	3.27432
Tf	NM_001013110	Transferrin	3.7506	3.10038
		Response to oxygen compounds		
Nqo1	NM_017000.2	NAD(P)H dehydrogenase, quinone 1	2.37531	2.33166
Mlc1	NM_001108105	Megalencephalic leukoencephalopathy with subcortical cysts 1	2.12194	2.55643
Gbp2	NM_133624.1	Guanylate nucleotide binding protein 2	2.68581	2.29991
Abcb1	NM_012623.2	ATP-binding cassette, sub-family B (MDR/TAP), member 1	2.98633	2.81256
Cebpb	NM_024125.3	CCAAT/enhancer binding protein (C/EBP), beta	2.45337	1.98883
Timp1	NM_053819.1	Tissue inhibitor of metalloproteinase 1	4.11365	2.61004
		Cell adhesion		
Fbln5	NM_019153.2	fibulin 5	−2.39974	−2.19017

Gene	Accession	Description	Fold change (treatment vs. control)	
			FSL1	Pam3CSK4
Gp38	NM_019358.1	Glycoprotein 38	2.46865	1.85081
Other				
Tnk2	NM_001008336.1	Tyrosine kinase, non-receptor, 2	−1.93094	−1.80097
Klhdc7a	NM_173427.2	Kelch domain containing domain 7a	1.86953	1.86771
Slc16a1	NM_012716.1	Solute carrier family 16 (monocarboxylic acid transporters), member 1	2.33029	2.01858
Prss35	NM_001008560.1	Protease, serine, 35	−1.84014	−2.06976
Hnrpa2b1	NM_001104613	Heterogeneous nuclear ribonucleoprotein A2/B1	2.40152	2.11111
Penk-rs	NM_017139.1	Preproenkephalin, related sequence	−2.37654	−2.23044
Olr557	NM_001000669.1	Olfactory receptor 557	2.08804	2.35568
Hdac4	NM_053449	Histone deacetylase 4	1.81091	1.99337

Table 2

Genes unique to cells.

Gene	Accession	Description	Fold change
Extracellular matrix			
Col11a1	XM_342325.2	Procollagen, type XI, alpha 1	−2.25628
Col3a1	NM_032085.1	Collagen, type III, alpha 1	−2.4782
Lum	NM_031050.1	Lumican	−2.36492
Cyp1b1	NM_012940	Cytochrome P450, family 1, subfamily b, polypeptide 1	1.87075
Col1a2	NM_053356.1	Procollagen, type I, alpha 2	−2.04869
Fbln1	NM_00112754 7	Fibulin 1	−2.01646
Col1a1	NM_053304	Collagen, type 1, alpha 1	−2.40183
Col5a2	NM_053488.1	Collagen, type V, alpha 2	−1.98384
Cell adhesion			
Spp1	NM_012881.1	Secreted phosphoprotein 1	2.09366
Ccdc80	NM_022543	Coiled-coil domain containing 80	−1.82219
Cd44	NM_012924.2	CD44 antigen	1.93749
Fam38a	NM_00107720 0	Piezo-type mechanosensitive ion channel component 1 (Piezol)	2.02991
Cx3cl1	NM_134455.1	Chemokine (C-X3-C motif) ligand 1	2.03788
Dab2	NM_024159.1	Disabled homolog 2 (Drosophila)	−1.89182
Cd63	NM_017125.2	CD63 antigen	2.03799
Cell differentiation			
Picalm	NM_053554.1	Phosphatidylinositol binding clathrin assembly protein	1.93321
Dbn1	NM_031024.1	Drebrin 1	1.88264
Rasip1	NM_001106261	Ras interacting protein 1	1.82286
Nkx2-2	NM_001191904	NK2 homeobox 2	−2.41304
Igf2	NM_031511.1	Insulin-like growth factor 2	−3.53454
Ppp3r1	NM_017309.2	Protein phosphatase 3, regulatory subunit B, alpha isoform (calcineurin B, type I)	2.26484
Rohn	NM_001010953.1	Ras homolog gene family, member N	−2.16807
Junb	NM_021836.2	Jun-B oncogene	1.82868
Myt1	NM_001108615	Myelin transcription factor 1	−1.95865
Gpc3	NM_012774.1	Glypican 3	−2.06978
Tnmd	NM_022290.1	Tenomodulin	−2.66899
Msn	NM_030863.1	Moesin	1.91146
Other			
Pcp4	NM_013002.2	Purkinje cell protein 4	−2.03656
Angptl4	NM_199115.2	Angiopoietin-like protein 4	1.8038

Gene	Accession	Description	Fold change
Rarres2	NP_001013445	Retinoic acid receptor responder (tazarotene induced) 2	−1.83247
Acvrinp1	NM_053621.1	Activin receptor interacting protein 1	1.82705
Ns5atp9	NM_201418.1	NS5A (hepatitis C virus) transactivated protein 9	−1.86284
Tcn2	NM_022534.1	Transcobalamin 2	−1.81345
Rgs4	NM_017214.1	Regulator of G-protein signaling 4	1.94574
Setd3	XM_216781	SET domain containing 3	1.82581
Atp1a2	NM_012505.1	ATPase, Na+/K+ transporting, alpha 2 polypeptide	−2.26933
Fmo1	NM_012792.1	flavin containing monooxygenase 1	−1.96393
Ptgds	NM_013015.2	Prostaglandin D2 synthase	−5.86134
Uxs1	NM_139336.1	UDP-glucuronate decarboxylase 1	1.82609
Dcn	NM_024129.1	Decorin	−2.84111
Waspip	NM_057192.2	Wiskott-Aldrich syndrome protein interacting protein	−2.08682
Gjb2	NM_001004099.1	Gap junction membrane channel protein beta 2	−1.80584
Ap2b1	NM_080583.1	Adaptor-related protein complex 2, beta 1 subunit	2.16441
Tbxa2r	NM_017054.1	Thromboxane A2 receptor	1.82802
Ogn	NM_001106103	Osteoglycin	−2.00267
Aspn	NP_001014030	Asporin	−1.99136
Cdc2a	NM_019296.1	Cell division cycle 2 homolog A (S. pombe)	−2.13298
Lonp1	NM_133404.1	Protease, serine, 15 (Prss15), mRNA.	2.04288
Hivep2	NM_024137	Human immunodeficiency virus type I enhancer binding protein 2	1.89602
Serping1	NM_199093.1	Serine (or cysteine) peptidase inhibitor, clade G, member 1	2.00974
Scrg1	NM_033499.1	Scrapie responsive gene 1	−2.13317
Pgd	XM_003754118	6-phosphogluconate dehydrogenase, decarboxylating-like	2.02041
Ccdc85b	XM_003749044	Coiled-coil domain containing 85B	1.90987
Zeb1	NM_013164	Zinc finger E-box binding homeobox 1	−1.84333
Cxcl16	NM_001017478	Chemokine (C-X-C motif) ligand 16	1.80757

Table 3

Genes unique to Pam_3CSK_4-treated cells.

Gene	Accession	Description	Fold change
Extracellular matrix			
Ctgf	NM_022266.1	Connective tissue growth factor	−2.06223
Lox	NM_017061	Lysyl oxidase	−2.38908
A2m	NM_012488.1	Alpha-2-macroglobulin	1.8568
Other			
Lpd	NM_134389.1	Lipidosin	1.80417
Sst	NM_012659.1	Somatostatin (Sst), mRNA.	−1.84121
Cldn17	NM_001107112.1	Claudin 17	1.8814
Cyp7b1	NM_019138	Cytochrome P450, family 7, subfamily b, polypeptide 1	1.94516